Available online at www.sciencedirect.com
ScienceDirect
Journal of Nuclear Materials 356 (2006) 189–197
journal of nuclear materials
www.elsevier.com/locate/jnucmat

Oxidation of steel T91 in flowing lead–bismuth eutectic (LBE) at 550 °C

C. Schroer *, Z. Voß, O. Wedemeyer, J. Novotny, J. Konys

Forschungszentrum Karlsruhe in der Helmholtz-Gemeinschaft, Institut fuer Materialforschung III, Hermann–von-Helmholtz–Platz 1, 76344 Eggenstein-Leopoldshafen, Germany

Abstract

This paper reports results of exposure experiments with martensitic steel T91 for 1200, 2998 and 5016 h in the CORRIDA loop. Owing to initial problems with the enrichment of oxygen in the circulating LBE, the conditions with respect to the oxygen activity (expressed as the activity of lead oxide, a_{PbO}) varied significantly. At 550 °C, oxidation is the only mode of material degradation for T91 in flowing LBE (2 m/s) when the oxygen activity corresponds to $10^{-4} \leqslant a_{PbO} \leqslant 10^{-2}$. The mean oxidation rate in the course of the first 1200 h approximates 0.13 mm/year. Lower oxygen activity in the LBE ($10^{-6} \leqslant a_{PbO} \leqslant 10^{-4}$) may be beneficial with respect to the oxidation rate, but undershooting a certain value around the threshold for Fe_3O_4 stability ($a_{PbO} = 10^{-5.2}$) poses the risk of liquid–metal attack accompanied by high local material consumption. The composition and structure of the oxide scales on the surface of T91 are analysed and a mechanism for scale growth initiating from oxide nuclei of various compositions is proposed.

1. Introduction

From a nuclear engineering point of view, liquid lead (Pb), bismuth (Bi) and the lead–bismuth eutectic (LBE) have unique properties and, therefore, were taken into consideration as a process medium for a number of applications in the use of nuclear energy. However, the incompatibility of Pb, Bi and their alloys in the liquid state with steels, the favoured construction materials for respective plants, is one of the prominent reasons for Pb–Bi alloys having not yet established themselves in nuclear technology, except in some niches. This incompatibility manifests itself in the dissolution of the main steel components like iron (Fe), chromium (Cr) and especially nickel (Ni) in the case of austenitic steels. A prominent role with respect to dissolving corrosion is assigned to oxygen which significantly lowers the dissolution rate when protective oxides form on the steel surface, but may promote plugging via oxide precipitation in colder parts of the plant [1].

Pb and LBE recently regained interest in connection with the development of accelerator-driven subcritical systems (ADS). Such systems are designed for the transmutation of plutonium, minor actinides and radioactive fission products with long half-life periods, which are separated from nuclear

* Corresponding author. Tel.: +49 (0)7247 82 4473; fax: +49 (0)7247 82 3956.
E-mail address: carsten.schroer@imf.fzk.de (C. Schroer).

0022-3115/$ - see front matter © 2006 Elsevier B.V. All rights reserved.
doi:10.1016/j.jnucmat.2006.05.009

waste in a preceding process (partitioning). Partitioning and subsequent transmutation is capable of significantly reducing the radio-toxicity of waste from nuclear power plants before final storage. In the proposed ADS concepts, Pb or LBE serves as a target for accelerated protons and delivers the neutrons which are necessary to maintain the transmutation. Additionally, the liquid alloy dissipates the heat released in the core of the system by transfer onto a secondary coolant in a heat exchanger. Adjusting the oxygen concentration (chemical potential) in the liquid metal to a level which is sufficiently high to allow for oxidation of the construction materials (steels) but much too low for formation of lead monoxide, PbO (the most stable solid oxide in the Pb–Bi system), should prevent dissolving corrosion without the risk of plugging.

In order to examine the applicability of the 9Cr1MoVNb-steel T91 (DIN W.-Nr. 1.4903) in an ADS operated with LBE as a target and primary coolant, this steel was exposed in the CORRIDA loop at the Karlsruhe Lead Laboratory (KALLA) to flowing Pb–Bi of practically eutectic composition (46 mass% Pb) at 550 °C. Oxygen is introduced into the liquid alloy via mass transfer from a gas with adjustable oxygen partial pressure. The chemical potential of oxygen achieved in the liquid metal is measured using oxygen sensors in selected positions along the loop. Results of exposures for up to 5000 h will be presented.

2. Experimental

2.1. Sample material and specimen preparation

Prior to machining of specimens for the exposure experiments, the T91 sample ($100 \times 100 \times 40$ mm) was austenitised at 1050 °C, cooled down and subsequently tempered at 750 °C. The parameters of this heat treatment are summarised in Table 1 along with the chemical analysis of the steel. From the heat-treated material, cylinders of dimensions $\varnothing 8 \times 35$ mm were cut and provided with an internal and external screw–thread at the top and bottom end, respectively. The threads allow a number of specimens to be joined, resulting in a specimen rod (normally consisting of 16 specimens of the diverse steels investigated) which is then introduced into one of the test-sections of the CORRIDA loop. The surface of the specimens was finished by turning and cleaned with acetone before introducing into the loop.

2.2. Materials testing in the CORRIDA loop

CORRIDA is a forced convection loop with a developed length of 36 m. All components are made of a 17–12 Cr–Ni steel (DIN W.-Nr. 1.4571). The hold-up volume of liquid Pb–Bi is approximately 1000 kg and, in the steady state, circulates at a mass-flow rate of 5.3 kg/s, resulting in a time necessary for one circulation of 190 s. A schematic illustration of the CORRIDA loop is shown in Fig. 1.

The circulation of the liquid metal is forced with an air-cooled electromagnetic pump which represents both the coldest (380 °C) and the lowest point along the loop (except for the dump tank). A counter-flow heat-exchanger and additional heaters following in the direction of the flow increase the temperature to 550 °C, the designated temperature in the two test-sections of the loop. The test-sections consist of vertical tubes with an inner diameter of 20 mm, i.e., the velocity with which the Pb–Bi passes the specimens is 2 m/s.

The concentration (chemical potential) of oxygen dissolved in the liquid metal is controlled in a tank (oxygen-control box; OCB) which is located past the test-sections in the direction of flow for hydrostatic reasons and is kept at 550 °C. The Pb–Bi flows through the OCB simultaneously with an oxygen-containing gas stream which is fed in above the liquid–metal surface (optionally via a lance immersed at the bottom of the OCB). The Pb–Bi absorbs oxygen when the chemical potential of oxygen in the liquid metal is lower than in the gas; in the case of reverse conditions, oxygen is released

Table 1
Composition of the T91 sample examined (in mass%) and heat-treatment parameters

Fe	Cr	Mo	Mn	Si	V	Cu	Ni	Nb	Co	Al
Bal.	9.44	0.850	0.588	0.272	0.196	0.0980	0.100	0.072	0.0156	0.007
	C	N	P	S		Zn	Sn	Ti	W	Ta
	0.075	n.a.	0.018	0.006		0.0043	0.004	0.0010	<0.003	<0.001

Heat treatment of $100 \times 100 \times 40$ mm sample: (1) 2 h at 1050 °C; furnace cooling down to 350 °C, followed by air-cooling; (2) 4 h at 750 °C; furnace cooling.

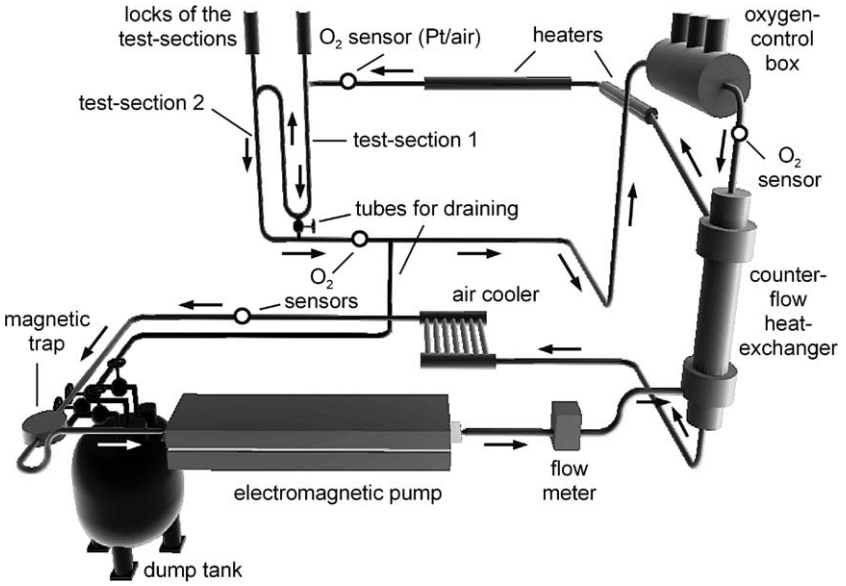

Fig. 1. Schematic illustration of the CORRIDA loop. The locks of the test-sections reside in a glove-box flushed with Ar, so as to minimise contamination of the Pb–Bi with oxygen during the exchange of specimens. The oxygen sensors employed along the loop work with Bi/Bi_2O_3 as oxygen-reference system except for the one which is indicated as a Pt/air sensor.

from the liquid. The instantaneous chemical potential (activity) of oxygen in the Pb–Bi is measured in selected positions along the loop (up- and downstream of the test-sections, downstream of the oxygen-control system and in the cold part of the loop) using zirconia solid-electrolyte sensors with platinum (Pt)/air or Bi/bismuth oxide (Bi_2O_3) as oxygen-reference systems [2,3]. After leaving the OCB, the Pb–Bi is cooled in the cold side of the counter-flow heat-exchanger and an additional air-cooler, before entering the pump again.

When the designated exposure time of specimens is reached, the pumping power is reduced so that the locks above the test-sections can be opened during operation. The specimen rods are removed from the test-sections, the respective specimens are substituted by new ones and the rods are then re-introduced into the loop. The specimen exchange is performed in a glove-box flushed with Ar, so as to prevent significant contamination of the Pb–Bi with oxygen. Slight oxidation of hot Pb–Bi adhering to the specimens (especially formation of PbO) is possible.

2.3. Testing conditions

The Pb–Bi alloy employed in the CORRIDA loop consists of 46 mass % Pb, which differs only slightly from the composition of the lead–bismuth eutectic (44.8 mass% Pb; Temp. = 125.5 °C). The Pb and Bi thermodynamic activities at 550 °C are $a_{Pb} = 0.370$ and $a_{Bi} = 0.462$, in comparison to 0.357 and 0.477 for LBE [4]. Since it is unlikely that the corrosion behaviour of steels in an alloy with 46 mass% Pb does significantly deviate from that in LBE, the abbreviation 'LBE' is also used for the alloy with 46 mass% Pb. The actual composition is used for calculations which require thermodynamic activities of the liquid–metal components.

The target for the enrichment of oxygen in the LBE was an oxygen (O_2) activity of 1.30×10^{-23} with reference to pure gaseous oxygen at 550 °C and 1 bar which corresponds to a H_2-to-H_2O partial pressure ratio of 0.04. This O_2 activity is significantly higher than the threshold for magnetite (Fe_3O_4) formation at 550 °C (1.53×10^{-27}) and falls below the threshold for PbO precipitation (3.15×10^{-17} for $a_{Pb} = 0.370$). The corresponding target value for the electromotive force (EMF) indicated by the Pt/air sensor which resides near the inlet of the first test-section is $E = 0.91$ V.

In liquid–metal technology, the reference state for the oxygen (O) activity is often chosen as the precipitation point of the most stable oxide of the liquid–metal components, i.e., PbO in the case of LBE, which simplifies the estimation of oxygen concentrations on the basis of Henry's law [5]. If doing so, the O activity has the same value as the PbO

activity, a_{PbO}. The signal of the Pt/air sensor at the inlet of the first test-section recorded in the course of the exposure of T91 and corresponding PbO activities in the LBE are summarised in Fig. 2.

At the onset of operating the CORRIDA loop, it was assumed that the designated oxygen activity in the LBE can be adjusted by introducing 500 standard-cm^3/min Ar–0.03 vol.% H_2 saturated with water at 4 °C (resulting in H_2:$H_2O = 0.04$) into the OCB, i.e., oxygen transfer is sufficiently fast and the exchanged mass is low, so that chemical equilibrium between the liquid alloy and the gas is achieved without significantly altering the gas composition. Fig. 2 shows that these assumptions are not fulfilled. The oxygen activity rapidly decreased (the EMF indicated by the sensor increased) during the first 100 h of operation due to oxygen consumption (oxidation of the steel specimens and especially of the construction material of the loop) which is not balanced by the transfer of oxygen into the LBE. The decrease of oxygen activity slowed down after 100 h, but values in the range of the target were achieved only after a maintenance interval (involving draining and refilling of the loop) which became necessary after approximately 1000 h. After resuming operation, the oxygen activity decreased again, more slowly than during the first operation period but steadily. Between approximately 2300 and 3500 h of effective operation, the oxygen activity in the LBE was in the range and below the minimum activity necessary for formation of Fe_3O_4, i.e., conditions favourable for Fe dissolution and therefore dissolving corrosion of steels arose. After 3500 h, oxygen transfer was enhanced by means of compressed air which was dosed periodically into the head-space of the OCB in addition to the continuous stream of humidified Ar–H_2. With this measure, the oxygen activity in the LBE was periodically raised to the target value when the threshold for Fe_3O_4 stability had been approached in consequence of oxygen consumption in the loop (Fig. 2; operating time from 3500 to 5000 h). Since then, the oxygen control system has been supplemented by a precision valve which allows for the introduction of a finely adjusted, continuous air stream in addition to humidified Ar–H_2. Thus, the oxygen activity can be kept in a sufficiently narrow range around the target value.

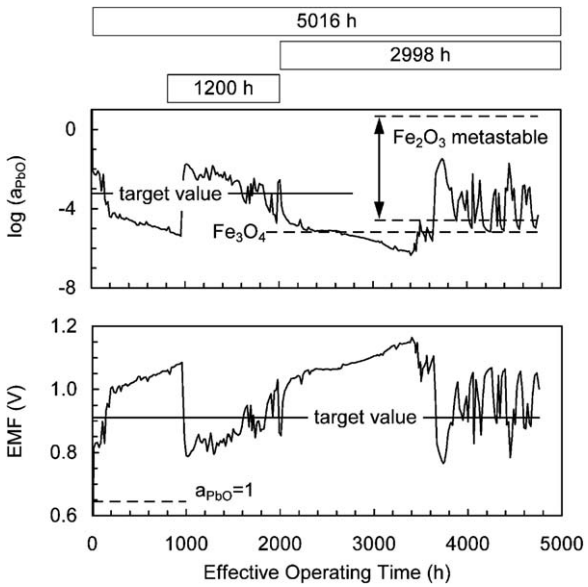

Fig. 2. Signal of the Pt/air sensor (EMF) residing near the inlet of the first test-section at 553 °C and corresponding PbO activity (a_{PbO}) for $a_{Pb} = 0.370$ as a function of operating time. Dashed lines mark the thresholds for the stability of oxides. Fe_2O_3 is metastable in the indicated range.

The bars in the upper part of Fig. 2 indicate the exposure periods for the specimens of T91 (one specimen for each exposure time) which are the subject of this paper. The specimen exposed for 1200 h experienced conditions in which Fe_3O_4 is stable, i.e., the desired conditions. The exposure for 2998 h started with low oxygen activity in the LBE and the threshold for Fe_3O_4 stability was reached after 400 h. Between ~750 and 1650 h of exposure (between 2750 and 3650 h of effective operation of the loop), the oxygen activity was below this threshold. Subsequently, the respective specimens experienced oxygen activities alternating between the target value and threshold for Fe_3O_4 stability. For the specimen which was exposed for 5016 h in the CORRIDA loop, the conditions with respect to the oxygen activity in the LBE were as discussed in the previous paragraph (varying conditions). Table 2 summarises the testing conditions.

2.4. Post-test examinations

For each exposure time, two half-cylindrical pieces of approximately 1 cm length were cut from the cylindrical specimen. One of these half-cylinders was used for the preparation of a longitudinal cross-section with adherent LBE. The other piece was repeatedly immersed in hot vegetable fat (160 °C) and rubbed with a cloth to remove adherent Pb–Bi from the surface. This part of the specimen was

Table 2
Summary of the testing conditions for T91

Duration (h)	Composition of the LBE			Temperature	Flow velocity
	Pb	Bi	O		
1200 2998 5016	46 mass% ($a_{Pb} = 0.370$)	54 mass% ($a_{Bi} = 0.462$)	$10^{-4} \leqslant a_{PbO} \leqslant 10^{-2}$ Mostly $10^{-6} \leqslant a_{PbO} \leqslant 10^{-4}$	550 °C	2.0 ± 0.2 m/s

See Fig. 2 for details on the prevailing oxygen activity.

analysed by means of X-ray diffraction (XRD) in order to determine the corrosion product phases (oxides) formed during the exposure. Additionally, two circular slices of approximately 2 mm thickness were cut from the specimen and used for the preparation of vertical cross-sections, one with adherent LBE and the other after cleaning in hot fat. The cross-sections were investigated in a light- and scanning electron microscope (SEM) supplemented by qualitative energy-dispersive X-ray micro-analysis (EDX).

The thickness of the corrosion scale on the steel surface was measured at 12 sites distributed uniformly along the circumference of the specimens in a light-microscope at a magnification of 500×, using the vertical cross-sections with adherent Pb–Bi. The thickness of distinguishable parts (layers) of the scale was also determined. Sites affected by substantial dissolving corrosion (liquid–metal attack) after exposure for 2998 and 5016 h were not included in these measurements but examined separately.

3. Results and discussion

In the case of all T91 specimens investigated after exposure at 550 °C in the CORRIDA loop, oxides of Fe and/or Fe–Cr mixed-oxides formed on the steel surface. However, as can be expected in view of the changing oxygen activity in the course of the experiments, the structure and development with time of the oxide scales are influenced by the temporary instability of certain oxides (e.g., Fe_3O_4) and the varying driving force for oxide growth in general. The specimen exposed for 1200 h experienced proper conditions throughout most of the exposure time and is therefore used as a basis for the presentation and discussion of the results. The other specimens which were exposed for longer times but under changing conditions (and exhibited some sites affected by liquid–metal attack) are analysed with respect to how the steel will behave when the oxygen activity in the LBE cannot be kept in the favourable range.

3.1. Structure and composition of oxide scales

An oxide scale typical for the oxidation of T91 in flowing LBE at 550 °C and oxygen activities well above the threshold for Fe_3O_4 stability is shown in Fig. 3. According to qualitative EDX analyses, the outer part of this scale is almost pure Fe oxide (with only small amounts of Cr) followed by an intermediate layer of Fe–Cr mixed-oxide. At the metal/scale interface, an only partly oxidised internal oxidation zone (IOZ) has established, exhibiting Cr-rich oxide precipitates along grain boundaries and also within the steel grains. Near the transition between the Fe–Cr mixed-oxide and the IOZ, a porous zone intersects the mixed-oxide layer. Looking closer at the interface between Fe-oxide and mixed-oxide, oxide particles which are more Cr-rich than their surroundings are observed. Such Cr-rich oxide particles are also found within the mixed-oxide layer, probably tracing the original grain boundaries of the steel. The microstructure of the mixed-oxide layer is still being investigated by means of Auger-electron spectroscopy and electron-microprobe analyses.

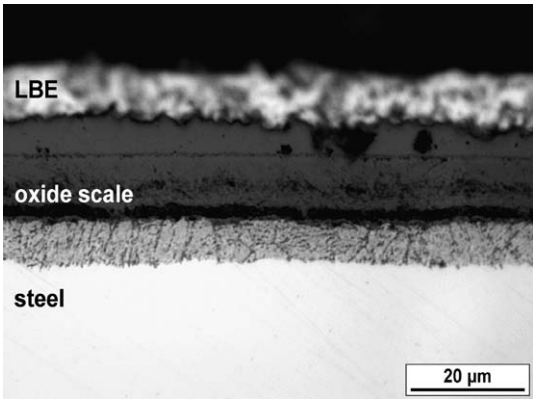

Fig. 3. Vertical cross-section of T91 after exposure for 1200 h at 550 °C in LBE. The oxygen activity in the LBE was well above the threshold for Fe_3O_4 stability for most of the exposure time. Light-optical micrograph.

The XRD-spectrum recorded from the surface of the oxide scale shows only peaks corresponding to cubic Fe–Cr oxides such as Fe_3O_4, Fe–Cr spinel and maghaemite (γ-Fe_2O_3), except for signals corresponding to Bi which remained on the surface after cleaning (Fig. 4). From these oxides, γ-Fe_2O_3 is metastable at the oxygen activities prevailing during the exposure for 1200 h (Fig. 2), i.e., γ-Fe_2O_3 may, in principle, form on the bare steel surface but is prone to decomposition into Fe_3O_4 and oxygen at an LBE/Fe_2O_3 interface (the same is true for haematite, α-Fe_2O_3). Therefore, the Fe-oxide in the outer part of the scale on T91 after the exposure for 1200 h most likely is Fe_3O_4, the least stable oxide in the Fe–O system which can coexist in chemical equilibrium with the LBE at the respective oxygen activities. The intermediate layer of Fe–Cr mixed oxide is Fe–Cr spinel, but, considering the composition of T91 and the results of qualitative EDX analyses, the Fe-to-Cr ratio is probably significantly higher than in stoichiometric spinel, as expressed by the chemical structure $Fe(Fe_xCr_{1-x})_2O_4$. The XRD-spectrum does not contain information on the oxides precipitated in the IOZ, but, from a thermodynamic viewpoint, these oxides must be more stable than the spinel forming the mixed-oxide layer and can be either a more Cr-rich spinel, chromia (α-Cr_2O_3) or an Fe–Cr mixed-oxide basing on Cr_2O_3.

Tökei et al. [6] showed that the composition of the oxides formed on a clean surface of T91 at 600 and 650 °C and low oxygen pressure (10^{-8}–10^{-11} bar) depends on the local Cr-content of the martensite laths and the surface segregation of silicon, phosphorous and nitrogen. They identified M_3O_4-type oxides as the principal corrosion product at 600 °C. The influence of segregation from the bulk of the steel which, e.g., results in local formation of silicon oxide (SiO_2) is more pronounced for higher temperature and lower oxygen pressure. In light of these findings, it is likely that the Cr-rich oxide particles at the $Fe_3O_4/Fe(Fe_xCr_{1-x})_2O_4$ interface are a remnant of the initial stage of oxidation in the LBE, during which oxide nuclei of type M_3O_4 with diverse Fe-to-Cr ratios formed on the steel surface. The, in comparison to the experiments by Tökei et al., very low oxygen activity in the LBE and fast Cr-diffusion along martensite lath boundaries and dislocation networks (which form during tempering of the martensite [7]) support the formation of Cr-rich oxides, in addition to near-surface Cr-carbides; also Cr-rich M_2O_3-oxides can originate in this initial stage. However, the high Fe-content of the steel and the lower solubility of Fe in LBE (~5 at. ppm at 550 °C [8]) in comparison to Cr (~15 at. ppm [9]) promote the formation of Fe-rich oxide nuclei.

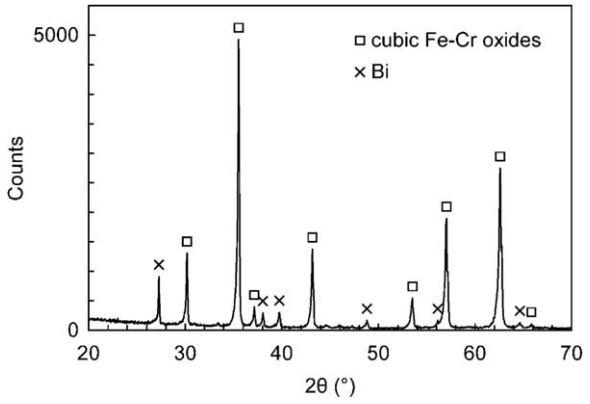

Fig. 4. XRD-spectrum recorded from the oxide-scale surface after exposure of T91 for 1200 h in the CORRIDA loop and removal of adherent LBE in hot fat.

Starting from oxide nuclei of various composition, a scale according to Fig. 3 results from outward growth (at the LBE/oxide interface) of Fe_3O_4 and inward growth (at the metal/oxide interface) of $Fe(Fe_xCr_{1-x})_2O_4$. The exceptionally Cr-rich oxide particles formed in the initial stage of oxidation do not grow significantly and remain at the original steel surface. Oxygen entering the scale is not completely consumed by growth of the spinel layer and causes internal oxidation accompanied by formation of Cr-rich oxides (of spinel-type or M_2O_3) where grain boundaries and dislocation networks allow for ingress of oxygen into the steel. Consequently, the spinel layer grows inwardly and consumes the IOZ, which, on its part, proceeds deeper into the steel. Fe diffuses outwardly through the spinel and promotes the continued Fe-oxide growth at the scale surface, whereas Cr is comparatively immobile and remains (predominantly) in the oxides within the original limits of the steel specimen. Considering that the Pilling–Bedworth ratio for the formation of Fe–Cr oxides of type M_3O_4 (Fe_3O_4, $FeCr_2O_4$) on ferritic steel is ~2 [10], the structure of the scale in Fig. 3 implies that approximately 25% of the consumed metal (mainly Fe) dissolves in the LBE or respective amounts of oxide are eroded by the flow simultaneously with oxidation of the steel; if all the metal consumed remained in the oxides on the steel surface, the thickness of the

outer Fe_3O_4 layer (averaging 5 μm in the case considered) would approximately equal the thickness of the inward growing spinel layer (averaging 10 μm in the case considered). Fe dissolution is influenced by the decreasing oxygen activity in the LBE during the exposure for 1200 h, and possibly does not occur if the oxygen activity was always around the target for the oxygen enrichment.

The oxide scales which are observed after exposure for 2998 and 5016 h under varying conditions with respect to the oxygen activity in the LBE are similar to the scale observed after exposure for 1200 h, with the exception that the outer Fe_3O_4 layer is completely missing after the exposure for 5016 h. After 2998 h, significant amounts of Fe_3O_4 are only locally present. The spinel layer exhibits comparatively compact sub-layers having possibly resulted from gaps which open due to intermittent cooling down during interruptions of the experiment for the exchange of other specimens and are refilled with oxide when the exposure at 550 °C is continued. The oxide particles in the IOZ show the tendency to coarsen with increasing exposure time and protrude into the steel especially along the prior austenite grain boundaries. A striking difference between the exposure at oxygen activities above the threshold for Fe_3O_4 formation and the exposure for 2998 h which started with oxygen activities around and below this threshold are domains of the steel surface covered with a thin (~1 μm), Cr-rich oxide scale; comparatively little internal oxidation occurred beneath this thin scale (Fig. 5). The formation of this rather protective oxide scale is promoted by the low oxygen activity at the beginning of the exposure, but the Cr-content of the steel is probably not high enough to establish a Cr-rich scale over the entire specimen surface. A closer look at the transition between the thick and thin domains of the oxide scale in Fig. 5 implies that the surface of the $Fe(Fe_xCr_{1-x})_2O_4$ layer approximates the original steel surface even if Fe_3O_4 is missing.

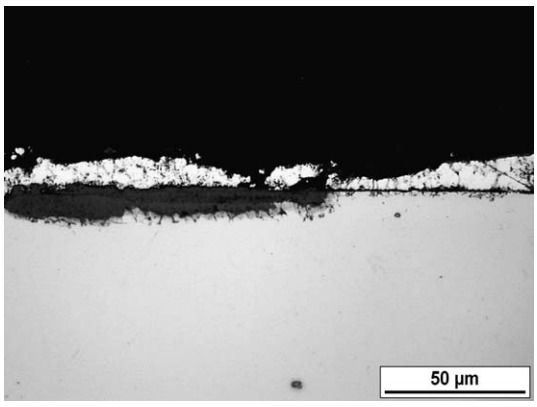

Fig. 5. Domains with thick and thin oxide scale on the surface of T91 after exposure for 2998 h under varying conditions with respect to the oxygen activity (temporarily below the threshold for Fe_3O_4 stability) in the LBE. Light-optical micrograph.

3.2. Oxidation rates

For the estimation of oxidation rates, it was assumed that the $Fe_3O_4/Fe(Fe_xCr_{1-x})_2O_4$ interface or, if Fe_3O_4 is missing, the surface of the spinel layer indicates the original position of the steel surface. This assumption is based on findings discussed in the previous section and especially on the results of experiments performed in flowing liquid lead with steels partly surface-alloyed with aluminium [11]. Accordingly, the metal recession (or depth of material degradation) is the sum of the thicknesses of the inward growing spinel layer and the IOZ. The metal recessions observed after the different exposure times and their distribution between the inward growing scale and IOZ are compiled in Fig. 6.

Although the measured metal recessions do not allow for determination of the oxidation kinetics

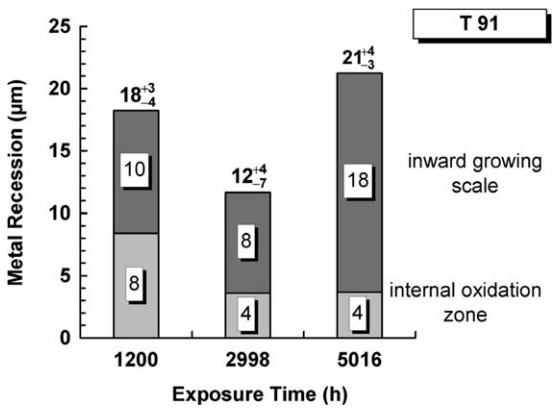

Fig. 6. Metal recession of T91 after exposure in the CORRIDA loop, as determined from the thickness of the inward growing part of the oxide scale and IOZ (respective mean values are given within the columns). The mean metal recession and the deviation of the maximum and minimum, respectively, of 12 measurements are stated above the columns. It should be emphasised that the specimens exposed for 1200, 2998 and 5016 h, respectively, experienced different conditions with respect to the oxygen activity in the LBE (cf. Fig. 3).

because of the varying conditions with respect to the oxygen activity in the LBE during the exposures, the single values can be used to estimate linear oxidation rates for the respective conditions. This linear oxidation rate is the metal recession due to scale formation plus simultaneous metal dissolution and/or erosion of oxides divided by the exposure time, and represents the mean rate of material degradation within this time period, disregarding that this oxidation rate possibly decreases with time, i.e, increasing scale thickness.

The metal recession after exposure for 1200 h corresponds to a linear oxidation rate of 0.13 mm/year which is a first estimate for the degradation of T91 at 550 °C in flowing LBE and oxygen activities above the threshold for Fe_3O_4 formation; approximately 25% results from Fe dissolution and/or erosion of Fe_3O_4 (cf. Section 3.1). For the exposures for 2998 and 5016 h under varying conditions with respect to the oxygen activity, the linear oxidation rate is 0.04 mm/year, i.e., significantly lower than for the exposure at higher mean oxygen activity. The transfer of metals into the LBE (dissolution, erosion of oxide) accounts for about 50% of this oxidation rate (no Fe_3O_4 on the scale surface) and, since it is most likely triggered by the inward growing part of the scale, is also lower than at higher mean oxygen activity.

It should be emphasised that the evaluated oxidation rates consider only the behaviour in the absence of liquid–metal attack. Such a mode of corrosion, which is accompanied by substantial metal dissolution, occurs at some sites on both specimens which were exposed to varying conditions with respect to the oxygen activity and exhibit low oxidation rates. The maximum depth of liquid–metal attack is ~190 μm after both 2998 and 5016 h, indicating that liquid–metal attack may have started at approximately the same absolute time, probably during the period of much too low oxygen activity around 3000 h of effective operation of the loop (Fig. 2).

4. Conclusions

A first series of experiments at 550 °C in the CORRIDA loop shows that, during exposure for 1200 h, oxidation is the only mode of material degradation for T91 in flowing LBE (2 m/s) when the prevailing oxygen activity in the LBE corresponds to $10^{-4} \leqslant a_{PbO} \leqslant 10^{-2}$. The mean oxidation rate (in terms of metal recession) in this time interval approximates 0.13 mm/year. The oxide scale consists of an outer Fe_3O_4 layer at the LBE/scale interface, a $Fe(Fe_xCr_{1-x})_2O_4$ layer which grew into the steel and an internal oxidation zone with Cr-rich oxide precipitates along prior austenite grain boundaries, martensite lath boundaries and probably also along near-surface dislocation networks. The part of metal which is transferred into the LBE by either metal (Fe) dissolution through the scale or erosion of Fe_3O_4 is estimated to be 25% of the overall material consumption.

When the oxygen activity in the LBE is mostly in a range corresponding to $10^{-6} \leqslant a_{PbO} \leqslant 10^{-4}$ and thus Fe_3O_4 is temporarily unstable ($a_{PbO} < 10^{-5.2}$), the oxidation rate is significantly lower. When the exposure starts with oxygen activities around the threshold for stability of Fe_3O_4, an exceptionally protective, probably Cr-rich scale may form. However, the Cr-content of T91 is too low and Cr-diffusion in the steel is respectively too slow to establish such a Cr-rich scale over the entire surface. Both the mean oxidation rate and the absolute amount of Fe transferred into the LBE seem to be lower the lower the oxygen activity in the LBE, so that a target for the oxygen enrichment in a range corresponding to $10^{-5} \leqslant a_{PbO} \leqslant 10^{-4}$ may be beneficial for technical applications. Undershooting a certain threshold (not necessarily exactly but around the threshold for Fe_3O_4 stability) poses the risk of liquid–metal attack, accompanied by high local material consumption.

All things considered, T91 shows promising (short-term) oxidation behaviour in flowing LBE at 550 °C and $10^{-4} \leqslant a_{PbO} \leqslant 10^{-2}$ with respect to the suppression of liquid–metal attack. Oxygen activities in the LBE corresponding to the lower edge of this range may be beneficial for technical applications, especially for achieving a satisfactory life-time of thin-walled components in plants operated with LBE as a process medium. Additional experiments are necessary to confirm oxidation rates and investigate the time-dependence of oxidation under more controlled conditions with respect to the oxygen activity in the LBE.

Acknowledgements

This work was performed in the framework of the Nuclear Safety Programme of the Forschungszentrum Karlsruhe. Special thanks go to E. Nold and R. Rösch (Institut fuer Materialforschung I, Forschungszentrum Karlsruhe) for examining the microstructure of oxide scales.

References

[1] J.R. Weeks, Nucl. Eng. Design 15 (1971) 363.
[2] J. Konys, H. Muscher, Z. Voß, O. Wedemeyer, J. Nucl. Mater. 296 (2001) 289.
[3] H. Muscher, J. Konys, Z. Voß, O. Wedemeyer, Measurement of oxygen activities in eutectic lead–bismuth by means of the EMF method; Report FZKA 6690, Forschungszentrum Karlsruhe GmbH, Germany, 2001.
[4] N.A. Gokcen, J. Phase Equilibria 13 (1992) 21.
[5] H.U. Borgstedt, C.K. Mathews, Applied Chemistry of the Alkali Metals, Plenum, New York, London, 1987, p. 78.
[6] Zs. Tökei, H. Viefhaus, H.J. Grabke, Appl. Surf. Sci. 165 (2000) 23.
[7] P.J. Ennis, A. Czyrska-Filemonowicz, Sadhana 28 (2003) 709.
[8] J.R. Weeks, A.J. Romano, Corrosion 25 (1969) 131.
[9] G. Rosenblatt, J.R. Wilson, The solubilities of several transition metals in liquid lead–bismuth eutectic, in: J.E. Draley, J.R. Weeks (Eds.), Corrosion by Liquid Metals, Plenum, New York, London, 1970, p. 469.
[10] N. Birks, G.H. Meier, Introduction to High Temperature Oxidation of Metals, Edward Arnold, London, 1983, p. 118.
[11] G. Müller, G. Schumacher, F. Zimmermann, J. Nucl. Mater. 278 (2000) 85.